

ChemComm

Accepted Manuscript



This is an *Accepted Manuscript*, which has been through the Royal Society of Chemistry peer review process and has been accepted for publication.

Accepted Manuscripts are published online shortly after acceptance, before technical editing, formatting and proof reading. Using this free service, authors can make their results available to the community, in citable form, before we publish the edited article. We will replace this *Accepted Manuscript* with the edited and formatted *Advance Article* as soon as it is available.

You can find more information about *Accepted Manuscripts* in the [Information for Authors](#).

Please note that technical editing may introduce minor changes to the text and/or graphics, which may alter content. The journal's standard [Terms & Conditions](#) and the [Ethical guidelines](#) still apply. In no event shall the Royal Society of Chemistry be held responsible for any errors or omissions in this *Accepted Manuscript* or any consequences arising from the use of any information it contains.



Blue Thermally Activated Delayed Fluorescence Materials Based upon Bis(phenylsulfonyl)benzene Derivatives†

Received 00th January 20xx,
Accepted 00th January 20xx

Ming Liu,^a Yuki Seino,^b Dongcheng Chen,^a Susumu Inomata,^b Shi-Jian Su,^{*a} Hisahiro Sasabe,^{*b} and Junji Kido^{*b}

DOI: 10.1039/x0xx00000x

www.rsc.org/

Two blue thermally activated delayed fluorescence molecules based on bis(phenylsulfonyl)benzene with very small singlet-triplet splitting energy were designed and synthesized by combining 3,6-di-*tert*-butylcarbazole with 1,4-bis(phenylsulfonyl)benzene and 1,3-bis(phenylsulfonyl)benzene, and a maximum external quantum efficiency of 11.7% was achieved for electroluminescent device.

Organic light-emitting diodes (OLEDs) have gained huge attention owing to their potential applications in both of new generation full-color flat-panel displays and new-generation solid-state lighting.¹ In the past two decades, incalculable efforts have been devoted to exploring new OLED emitters, and great success has been achieved, particularly, for heavy metal complex phosphorescent emitters. An internal quantum efficiency (IQE) of 100% can be obtained by reasonable design of device configurations.² However, most of these phosphorescent emitters contain rare metal elements such as iridium, platinum, and osmium which make them expensive and unfavorable to commercial application in flat-panel display and lighting sources. Especially for blue OLEDs, it is difficult to obtain wide energy gap phosphors, and their short device lifetimes are not suitable for commercial application.³ To address these issues, researchers are recently focusing on development of new type fluorescent materials, aiming to the utilization of triplet excitons in low-cost OLEDs based on metal-free fluorescent materials.⁴ Thermally activated delayed fluorescence (TADF) process is effective and amazingly attractive because there is a nearly 100% theoretical exciton utilization could be harvested by the approach of thermal energy-assisted intersystem crossing (ISC) process from the lowest triplet excited state (T_1) to the singlet excited state (S_1).⁵ Thermal

activation energy allow the accumulated triplet excitons at T_1 of the TADF emitter transfer to S_1 via ISC process and then eventually occur radiative decay to form fluorescent emission. To facilitate this up-conversion process, a small enough singlet-triplet splitting energy (ΔE_{ST}) is much critical for the emitter. It is advisable to construct a donor-acceptor (D-A) type structure with steric hindrance between the electron donor and electron acceptor moieties and thus spatial separation of the lowest unoccupied molecular orbitals (LUMOs) and highest occupied molecular orbitals (HOMOs), which is a significant factor in the realization of a small ΔE_{ST} for efficient TADF emitters. Adachi's group have reported a number of diphenylsulfone (DPS) containing compounds exhibited TADF characteristics. Particularly, 3,6-di-*tert*-butylcarbazole (DTC) substituted molecule DTC-DPS has been proved to perform excellently in OLED device, which achieved a high external quantum efficiency (EQE) and even a deep blue emission.⁷ In their further investigations, a series of modified DPS compounds have been synthesized and studied thoroughly. Using substituents of 5-phenyl-5,10-dihydrophenazine, phenoxazine, 9,9-dimethyl-9,10-dihydroacridine, or 3,6-dimethoxycarbazole to replace 3,6-di-*tert*-butylcarbazole on DPS led to changes of emission light, ΔE_{ST} , TADF lifetime, and also device performance.⁸ The oxygen of the sulfonyl group have significant electronegativity, which result in electron-withdrawing nature of sulfonyl. In addition, the sulfonyl group of DPS exhibits a tetrahedral geometry, which limit conjugation of the compounds.⁹ As thus, DPS has been turned out to be the most famous and typical electron acceptor component for TADF molecules in recent years. Generally, the compounds based on DPS possess a large twisted conformation between the phenyl ring and the electron donor, such as carbazole, acridine, and phenoxazine, leading to effective separation of frontier molecular orbitals and thus a comparatively small ΔE_{ST} . But for the blue TADF emitters based on DPS previously reported, their ΔE_{ST} values are relative larger than those of the green and yellow TADF molecules (for instance, 0.32 eV of DTC-DPS) to cause inefficient ISC process from T_1 to S_1 . While a smaller ΔE_{ST} could be achieved via adjusting the π -conjugation length and the electronic properties of the donor and acceptor moieties, we consider that if inserting one more phenyl sulfone into the DPS acceptor core could prospectively tune the electronic property and

^a State Key Laboratory of Luminescent Materials and Devices, Institute of Polymer Optoelectronic Materials and Devices, South China University of Technology, Guangzhou, 510640, P. R. China. E-mail: mssjsu@scut.edu.cn (S.-J. Su).

^b Department of Organic Device Engineering, Research Center for Organic Electronics (ROEL), Yamagata University, Yonezawa, 992-8510, Japan.

E-mail: h-sasabe@yz.yamagata-u.ac.jp (H. Sasabe); kid@yz.yamagata-u.ac.jp (J. Kido).

† Electronic Supplementary Information (ESI) available. See DOI: 10.1039/x0xx00000x

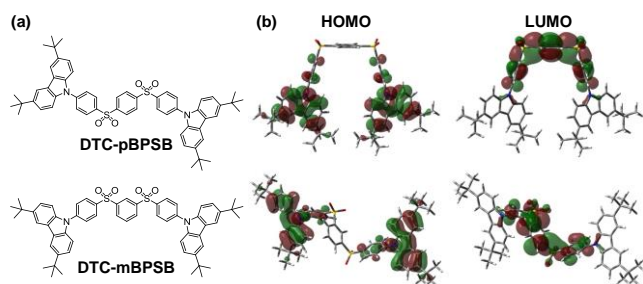


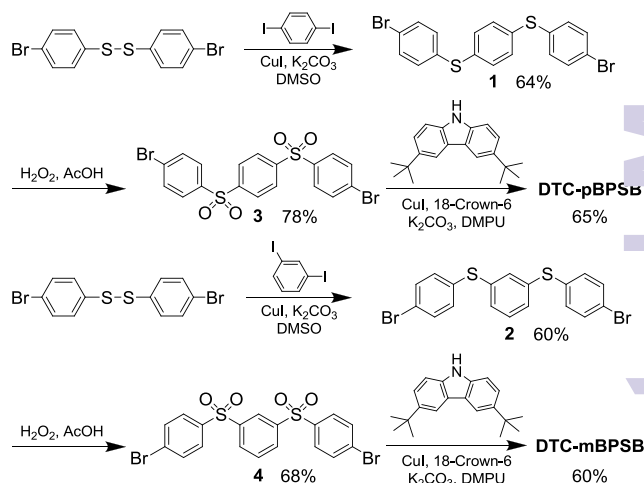
Fig. 1 (a) Molecular structures and (b) calculated frontier orbitals of HOMOs and LUMOs of DTC-mBPSB and DTC-pBPSB.

preserve the intrinsic triplet energy level. Consequently, a further decreased ΔE_{ST} could be attained.

In this communication, we describe the design, synthesis, comprehensive material properties and device performances of new blue TADF molecules of DTC-pBPSB and DTC-mBPSB based on two bis(phenylsulfonyl)benzene (BPSB) isomers with different configurations (1,4-bis(phenylsulfonyl)benzene and 1,3-bis(phenylsulfonyl)benzene), which possess two sulfonyl groups as electron acceptor and 3,6-di-*tert*-butylcarbazole as electron donor (Fig. 1(a)). Results show that the introduction of double sulfonyl system lead to molecules showing smaller ΔE_{ST} in comparison with their single sulfonyl counterpart, DTC-DPS. And DTC-pBPSB which adopts *para*-configuration of BPSB exhibited bathochromic-shift in emission spectrum but significantly higher device efficiency than its *meta*-isomer and single sulfonyl counterpart DTC-DPS.

The synthetic routes of DTC-pBPSB and DTC-mBPSB are outlined in Scheme 1, and details are given in electronic supplementary information (ESI). The pivotal precursors **3** and **4** were synthesized from the reactions of 1,2-bis(4-bromophenyl)disulfane with 1,4-diiodobenzene and 1,3-diiodobenzene, respectively, through three steps with considerable yields and were finally reacted with 3,6-di-*tert*-butyl-9-*H*-carbazole via common copper-catalyzed Ullmann reaction to give the target compounds. To evaluate their geometrical structure, frontier molecular orbitals, and energy band gaps, density functional theory (DFT) calculations were performed with B3LYP/6-31G(d,p) basis set by using Gaussian 09W program, and the electron densities of HOMOs and LUMOs of these two BPSB molecules are

depicted in Fig. 1(b).¹⁰ There are large torsion angles of 47.9° and 48.2° between the side phenyl rings of BPSB and the carbazole plane in the optimized geometries of DTC-pBPSB and DTC-mBPSB, respectively. And it can be found that the calculated HOMOs and LUMOs of these two molecules are separately distributed on the carbazole units and the BPSB segments, respectively, implying their strong charge transfer (CT) character which in turn would then contribute to small singlet-triplet splitting energy. Results of the excited state energies obtained by time-dependent density functional theory (TD-DFT) simulation with M062X/6-311G(d,p) basis set predict ΔE_{ST} values of 0.19 and 0.26 eV for DTC-pBPSB and DTC-mBPSB, respectively, and these values are distinctly less than 0.62 eV



Scheme 1 Synthetic routes for DTC-pBPSB and DTC-mBPSB.

of the earlier reported single sulfonyl compound, DTC-DPS. It is also need to point out that the pBPSB-based compound was predicted to exhibit narrower energy band gap (E_g) and smaller excited energy (singlet and triplet) than its mBPSB isomeric counterparts. That is due to the *meta*-configuration gives rise to a shorter effective conjugation length and weaker electron-withdrawing ability of the acceptor core.

DTC-pBPSB and DTC-mBPSB showed good thermal stability as indicated by the decomposition temperatures (T_d , corresponding to

Table 1 Physical properties and calculated energy levels of the compounds.

Compound	Experimental							Calculated			
	$T_d^{(a)}$ [C°]	λ_{abs} (solution) (b) [nm]	λ_{abs} (film) (c) [nm]	λ_{em} (solution) (b) [nm]	λ_{em} (film) ^(c) [nm]	$E_g^{opt(d)}$ [eV]	IP/EA ^(e) [eV]	HOMO/ LUMO ^(f) [eV]	$E_S^{(g)}$ [eV]	$E_T^{(g)}$ [eV]	$\Delta E_{ST}^{(g)}$ [eV]
DTC-pBPSB	427	295, 363	296, 347	446	474	2.85	-5.50/-2.65	-5.56/-2.11	3.06	2.87	0.19
DTC-mBPSB	403	293, 348	295, 348	422	444	2.98	-5.47/-2.49	-5.47/-1.88	3.19	2.93	0.26
DTC-DPS	-	290, 342 ^(h)	-	404 ^(h)	-	3.29 ^(h)	-5.81/-2.52 ^(h)	-5.04/-1.04	3.49	2.87	0.62

(a) Decomposition temperature (T_d) (5% weight loss); (b) UV-vis absorption and PL bands in toluene solutions at room temperature; (c) UV-vis absorption and PL peaks in neat thin films; (d) Optical energy band gaps (E_g^{opt}) estimated from the absorption edge in thin films; (e) Ionization potentials (IPs) of DTC-pBPSB and DTC-mBPSB determined from cyclic voltammetry and electron affinities (EAs) estimated from IPs and E_g^{opt} s; (f) HOMO and LUMO energy levels from the DFT calculations with B3LYP/6-31G(d,p) basis set by using Gaussian 09W program. [g] Energy of the first singlet and triplet state as well as ΔE_{ST} which obtained by time-dependent density functional theory (TD-DFT) calculations (M062X/6-311G(d,p), Gaussian 09W). (h) Data from the earlier literature.⁷

5% weight loss) above 400 °C which were obtained from thermogravimetric analyses (TGA), and such values are high enough for application in electroluminescent devices (Fig. S1). Cyclic voltammetry (CV) was used to estimate ionization potentials (IPs) of the current BPSB molecules.¹¹ Both of them displayed a quasi-reversible oxidative wave, which could be attributed to the oxidation of the electron donor carbazole units (Fig. S2). As estimated from the onset oxidation potentials (E_{ox} vs. ferrocene/ferrocenium), IPs of DTC-pBPSB and DTC-mBPSB are almost the same (-5.50 and -5.47 eV, respectively) despite their different configurations. Ultraviolet-visible (UV-vis) absorption and photoluminescence (PL) spectra of DTC-pBPSB and DTC-mBPSB in toluene solution are shown in Fig. 2 (a). Compared with its isomeric counterpart, DTC-pBPSB not only displays a broader intramolecular charge transfer (ICT) band located at ~370 nm, but also exhibits a stronger, lower energy peak at ~290 nm in the UV-vis absorption spectrum. DTC-mBPSB is highly emissive in deep blue region which is 25 nm hypochromatic shifted relative to DTC-pBPSB. These outcomes are well consistent with the theoretical calculation. From the onset of absorptions in thin film state, optical energy band gaps (E_g^{opt}) of DTC-pBPSB and DTC-mBPSB were estimated to be 2.85 and 2.98 eV, respectively, and their electron affinities (EAs) were estimated to be -2.65 and -2.49 eV from their IPs and E_g^{opt} s, respectively. Their PL spectra in dichloromethane at 77 K are shown in Fig. S3. The developed BPSB molecules display structureless emission band at low temperature. According to the onset of fluorescence (0 ms delay) and phosphorescence (1 ms delay) spectra, ΔE_{ST} values of DTC-pBPSB and DTC-mBPSB were respectively estimated to be only 0.05 and 0.24 eV. Such small ΔE_{ST} values prove the design strategy of the BPSB compounds as potential TADF emitters is effective.

To further certify their TADF character, transient PL decay curves of these two fluorophors in chloroform solution were obtained (Fig. S4). Under atmosphere, neither one of DTC-pBPSB and DTC-mBPSB shows long lifetime decay component. In such conditions, their photoluminescence quantum yields (PLQY) were measured to be 39.3 and 48.5%, respectively. However, in oxygen-free solutions, it can be seen that a fast decay is followed by a delayed component, which could be attributed to traditional fluorescence and TADF, respectively. Owing to the contribution of TADF, their PLQYs in chloroform solution increased to 56.3 and 69.3%, respectively. When doped into bis[2-(diphenylphosphino)phenyl]ether oxide (DPEPO) in a concentration of 10 wt%, DTC-pBPSB displays an emission peak at 461 nm, and DTC-

mBPSB is emissive in deep blue region with a peak of 434 nm (Fig. S5). As depicted in Fig. 2 (b), similar to that in solution, the transient PL decay curves of DTC-pBPSB and DTC-mBPSB co-deposited with DPEPO also present a prompt fluorescence component and a delayed TADF component. The lifetimes of the delayed components were fitted to be 1.23 and 1.16 μ s with proportion of 13.0% and 6.0% for DTC-pBPSB and DTC-mBPSB, respectively. In addition, DTC-pBPSB and DTC-mBPSB co-deposited with DPEPO show high PLQY values of 66.6 and 71.0%, respectively. As thus, the rate constants of ISC ($T_1 \rightarrow S_1$) were calculated to be 8.2×10^4 and 3.9×10^4 s^{-1} , and the rate constants of ISC ($S_1 \rightarrow T_1$) were calculated to be 3.4×10^6 and 2.4×10^6 s^{-1} for DTC-pBPSB and DTC-mBPSB, respectively. As a result of a large ΔE_{ST} , DTC-mBPSB shows less TADF component, smaller rate constants as well as harder ISC process from T_1 to S_1 than its *para*-isomer DTC-pBPSB.

In order to probe their electroluminescent properties, OLED devices were fabricated and investigated in a configuration of ITO/NPB (30 nm)/TCTA (20 nm)/CzSi (10 nm)/10 wt% BPSB compound/DPEPO (20 nm)/DPEPO (10 nm)/TPBI (30 nm)/LiF (1 nm)/Al. In which NPB, TCTA, CzSi and TPBI are abbreviations of *N,N'*-diphenyl-*N,N'*-bis(1-naphthyl)-1,10-biphenyl-4,4'-diamine, 4,4',4''-tri(*N*-carbazolyl)triphenylamine, 9-(4-*tert*-butylphenyl)-3,6-bis(triphenylsilyl)-9*H*-carbazole, and 1,3,5-tris(*N*-phenylbenzimidazol-2-yl)benzene, respectively. The device characteristics are shown in Fig. 3 and Fig. S6. EL spectra of these devices present similar features to their PL ones, and only true emissions from the emitters were detected, indicating that the charge recombination region was confined in the emitting layer and complete energy transfer from the host to the emitters was achieved. The device based on DTC-mBPSB exhibited deep blue electroluminescence with CIE coordinates of (0.15, 0.08) and a maximum current efficiency (CE) of 4.4 $cd A^{-1}$, corresponding to an EQE of 5.5%. While the device based on DTC-pBPSB delivered better device efficiencies, an EQE of 11.7% and a CE of 19.4 $cd A^{-1}$, and it can be ascribed to its relatively smaller ΔE_{ST} and easier ISC process from T_1 to S_1 . Due to the stronger ICT effect of DTC-pBPSB, it exhibits a sky-blue EL with CIE coordinates of (0.18, 0.19). In this device architecture, the deep HOMO energy level and poor hole transport capacity of the DPEPO host may make against to the balance of charge transport/injection and thus only moderate efficiency. In addition, it is an imperfection that the devices reported here are similar to the DTC-DPS based device which displayed significant efficiency roll-off as reported by Adachi *et al.* Optimization of the

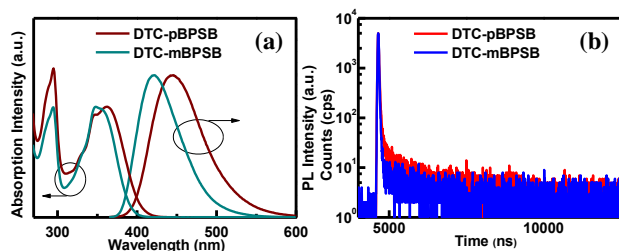


Fig. 2 (a) UV-vis absorption and PL spectra of DTC-mBPSB and DTC-pBPSB in toluene solution. (b) Transient PL decay curves of DTC-pBPSB and DTC-mBPSB co-deposited with DPEPO in a concentration of 10 wt% at room temperature.

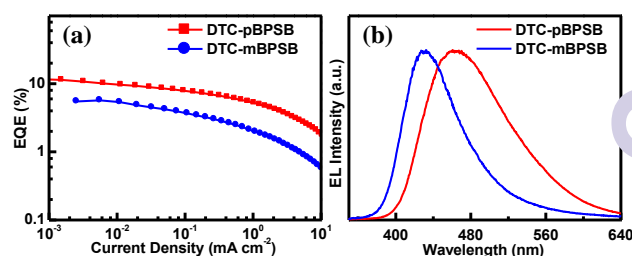


Fig. 3 (a) EQE versus current density characteristics and (b) EL spectra of the electroluminescence devices with an EML of 10 wt% DTC-pBPSB and DTC-mBPSB doped into DPEPO.

device structure for application of blue TADF emitters is expected to relieve this poser. Moreover, further design and development of new BPSB based emitters are in prospect to tune the emission light, ΔE_{ST} , TADF lifetime and acquire more excellent device performance. We also fabricated a control device containing DTC-DPS as a blue emitter for comparison. It came out that the EQE value of the device based on DTC-DPS is very close to that of the device based on DTC-mBPSB, but is only a half of that of the device based on DTC-pBPSB (Fig. S6). The current results indicate that BPSB could act as promising acceptor unit for developing efficient TADF emitters.

In summary, two BPSB-based isomers with different configurations were successfully designed, synthesized and applied as novel blue TADF emitters due to their low singlet-triplet exchange energies of 0.05 and 0.24 eV. DTC-mBPSB with 1,3-bis(phenylsulfonyl)benzene as the core exhibited a deep blue emission and an EQE of 5.5%. In contrast, DTC-pBPSB with 1,4-bis(phenylsulfonyl)benzene core exhibited a slightly red-shifted EL spectrum but superior EQE above 10%. Compared with the general DPS building block, it can be expected that further improved performance could be obtained by utilizing BPSB to construct novel TADF light-emitting materials.

The authors greatly appreciate the financial support from the Ministry of Science and Technology (2015CB655003 and 2014DFA52030), the National Natural Science Foundation of China (91233116 and 51073057), the Ministry of Education (NCET-11-0159), and the Guangdong Natural Science Foundation (S2012030006232).

Notes and references

- (a) C. W. Tang and S. A. VanSlyke, *Appl. Phys. Lett.*, 1987, **51**, 913; (b) J. Kido, M. Kimura and K. Nagai, *Science*, 1995, **267**, 1332; (c) S. Reineke, F. Lindner, G. Schwartz, N. Seidler, K. Walzer, B. Lussem and K. Leo, *Nature*, 2009, **459**, 234.
- (a) C. Adachi, M. A. Baldo, M. E. Thompson and S. R. Forrest, *J. Appl. Phys.*, 2001, **90**, 5048; (b) S. J. Su, H. Sasabe, T. Takeda and J. Kido, *Chem. Mater.*, 2008, **20**, 1691; (c) A. Kohler, J. S. Wilson and R. H. Friend, *Adv. Mater.*, 2002, **14**, 701; (d) H. Yersin and J. Strasser, *Coordin. Chem. Rev.*, 2000, **208**, 331.
- (a) H. Sasabe, J. Takamatsu, T. Motoyama, S. Watanabe, G. Wagenblast, N. Langer, O. Molt, E. Fuchs, C. Lennartz and J. Kido, *Adv. Mater.*, 2010, **22**, 5003; (b) T. Fleetham, G. J. Li, L. L. Wen and J. Li, *Adv. Mater.*, 2014, **26**, 7116.
- (a) J. Y. Hu, Y. J. Pu, F. Satoh, S. Kawata, H. Katagiri, H. Sasabe and J. Kido, *Adv. Funct. Mater.*, 2014, **24**, 2064; (b) C. J. Chiang, A. Kimyonok, M. K. Etherington, G. C. Griffiths, V. Jankus, F. Turksoy and A. P. Monkman, *Adv. Funct. Mater.*, 2013, **23**, 739; (c) L. Yao, S. T. Zhang, R. Wang, W. J. Li, F. Z. Shen, B. Yang and Y. G. Ma, *Angew. Chem. Int. Ed.*, 2014, **53**, 2119.
- (a) H. Uoyama, K. Goushi, K. Shizu, H. Nomura and C. Adachi, *Nature*, 2012, **492**, 234; (b) K. Goushi, K. Yoshida, K. Sato and C. Adachi, *Nat. Photonics*, 2012, **6**, 253; (c) A. Endo, K. Sato, K. Yoshimura, T. Kai, A. Kawada, H. Miyazaki and C. Adachi, *Appl. Phys. Lett.*, 2011, **98**, 083302. (d) D. D. Zhang, L. Duan, C. Li, Y. L. Li, H. Y. Li, D. Q. Zhang and Y. Qiu, *Adv. Mater.*, 2014, **26**, 5050.
- (a) Y. Tao, K. Yuan, T. Chen, P. Xu, H. H. Li, R. F. Chen, C. Zheng, L. Zhang and W. Huang, *Adv. Mater.*, 2014, **26**, 7931; (b) G. Mehes, H. Nomura, Q. S. Zhang, T. Nakagawa and C. Adachi, *Angew. Chem. Int. Ed.*, 2012, **51**, 11311; (c) T. Nakagawa, S. Y. Ku, K. T. Wong and C. Adachi, *Chem. Commun.*, 2012, **48**, 9580. (d) H. Wang, L. S. Xie, Q. Peng, L. Q. Meng, Y. Wang, Y. P. Yi and P. F. Wang, *Adv. Mater.*, 2014, **26**, 5198.
- Q. S. Zhang, J. Li, K. Shizu, S. P. Huang, S. Hirata, H. Miyazaki and C. Adachi, *J. Am. Chem. Soc.*, 2012, **134**, 14706.
- (a) Q. S. Zhang, B. Li, S. P. Huang, H. Nomura, H. Tanaka and C. Adachi, *Nat. Photonics*, 2014, **8**, 326; (b) S. H. Wu, M. Aonuma, Q. S. Zhang, S. P. Huang, T. Nakagawa, K. Kuwabara and C. Adachi, *J. Mater. Chem. C*, 2014, **2**, 421.
- Y. C. Li, Z. H. Wang, X. L. Li, G. Z. Xie, D. C. Chen, Y. F. Wang, C. C. Lo, A. Lien, J. B. Peng, Y. Cao and S. J. Su, *Chem. Mater.*, 2015, **27**, 1100.
- M. J. Frisch, G. W. Trucks, H. B. Schlegel, G. E. Scuseria, M. A. Robb, J. R. Cheeseman, G. Scalmani, V. Barone, B. Mennucci, G. A. Petersson, H. Nakatsuji, M. Caricato, X. Li, H. P. Hratchian, A. F. Izmaylov, J. Bloino, G. Zheng, J. L. Sonnenberg, M. Hada, M. Ehara, K. Toyota, R. Fukuda, J. Hasegawa, M. Ishida, T. Nakajima, Y. Honda, O. Kitao, H. Nakai, T. Vreven, J. A. Montgomery, Jr., J. E. Peralta, F. Ogliaro, M. Bearpark, J. Heyd, E. Brothers, K. N. Kudin, V. N. Staroverov, R. Kobayashi, J. Normand, K. Raghavachari, A. Rendell, J. C. Burant, S. S. Iyengar, J. Tomasi, M. Cossi, N. Rega, J. M. Millam, M. Klene, E. Knox, J. B. Cross, V. Bakken, C. Adamo, J. Jaramillo, R. Gomperts, R. E. Stratmann, O. Yazyev, A. J. Austin, R. Cammi, C. Pomelli, J. W. Ochterski, R. L. Martin, K. Morokuma, V. G. Zakrzewski, G. A. Voth, P. Salvador, J. J. Dannenberg, S. Dapprich, A. D. Daniels, O. Farkas, J. B. Foresman, J. V. Ortiz, J. Cioslowski and D. J. Fox, Gaussian 09, Gaussian Inc., Wallingford, CT, 2009.
- J. Pommerehne, H. Vestweber, W. Guss, R. F. Mahrt, H. Bässler, M. Porsch, J. Daub, *Adv. Mater.*, 1995, **7**, 551.